environments

MDPI

Article

Aptamer-Functionalized Magnetic Nanoparticles for Rapid Isolation of Environmental *Escherichia coli*

Zulema Herazo-Romero [1], Wendy Yulieth Royero-Bermeo [2], Miguel Octavio Pérez-Navarro [1], Miryan Margot Sánchez-Jiménez [3] and Juan David Ospina-Villa [3,*]

[1] Bioscience Group, Faculty of Health Sciences, Institución Universitaria Colegio Mayor de Antioquia (IUCMA), Medellín 50035, Colombia; ameluzhero1504@outlook.com (Z.H.-R.)
[2] Universidad CES, Medellín 50035, Colombia
[3] Instituto Colombiano de Medicina Tropical, Universidad CES (ICMT-CES), Sabaneta 055450, Colombia; msanchez@ces.edu.co
* Correspondence: jospina@ces.edu.co; Tel.: +57-44440555 (ext. 2537)

Abstract

Access to safe water remains a vital public health challenge, especially in low- and middle-income countries like Colombia, where untreated sources lead to severe diarrheal diseases in children under five. *Escherichia coli* (*E. coli*), a key indicator of fecal contamination, is often detected using culture-based methods that are time-consuming and rely on specialized infrastructure. To overcome these limitations, we developed an aptamer-based isolation system targeting environmental *E. coli*. Aptamers were obtained using a Cell-SELEX protocol, and after six enrichment rounds, two candidates—APT-EC-1 and its truncated version APT-EC-MUT—were synthesized and attached to carboxyl-functionalized magnetic nanoparticles (MNP-COOH). Both complexes demonstrated a strong binding affinity and high specificity, successfully isolating *E. coli* from environmental and ATCC reference strains in the laboratory. Sensitivity tests detected E. coli at dilutions up to 1:10,000, showing reliable performance. In early in-field testing with environmental water samples, APT-EC-1 consistently identified *E. coli* colonies, while APT-EC-MUT struggled with low bacterial levels, illustrating performance differences. These findings demonstrate the promise of aptamer-functionalized MNPs as the basis for quick, affordable, and portable biosensors for water quality testing, especially in resource-scarce areas. Future efforts will add colorimetric or electrochemical readouts to allow real-time, on-site detection of fecal contamination.

Keywords: aptamers; Cell-SELEX; *E. coli*; pull-down; water quality monitoring; biosensor

Academic Editor: Meilin Wu

Received: 7 August 2025
Revised: 5 September 2025
Accepted: 9 September 2025
Published: 18 September 2025

Citation: Herazo-Romero, Z.; Royero-Bermeo, W.Y.; Pérez-Navarro, M.O.; Sánchez-Jiménez, M.M.; Ospina-Villa, J.D. Aptamer-Functionalized Magnetic Nanoparticles for Rapid Isolation of Environmental *Escherichia coli*. *Environments* **2025**, *12*, 329. https://doi.org/10.3390/environments12090329

1. Introduction

Water is a vital resource for life, essential for human health, daily activities, agriculture, and industry. Securing access to safe drinking water is a global priority, as highlighted in Sustainable Development Goal 6, which calls for universal access to clean water and adequate sanitation [1]. However, ensuring drinking water safety remains a major public health challenge. In 2022, approximately 2.2 billion people lacked access to safely managed water, and 115 million did not even have basic services; additionally, 3.5 billion depended on sanitation systems that did not adequately treat human waste [2]. Poor water management contributes to contamination by heavy metals, toxic chemicals, agricultural runoff, and pathogenic microorganisms, leading to gastrointestinal diseases, chronic illnesses, and certain types of cancer [3,4]. Among these pollutants, microorganisms are particularly worrisome because they can cause acute infections that spread rapidly. Human activities such

as excretion, urination, and farming further intensify microbiological pollution, increasing disease risk through both ingestion and direct contact with contaminated water [5,6].

Monitoring microbiological water quality is therefore essential. Total coliforms and *Escherichia coli* (*E. coli*) are commonly used as indicators because they are closely linked to fecal contamination, are cost-effective to detect, and indicate the effectiveness of treatment [7]. *E. coli*, a rod-shaped bacterium from the Enterobacteriaceae family, is prevalent in human waste and serves as a reliable contamination marker [8]. Its pathogenic strains, especially diarrheagenic types, are leading causes of diarrhea, particularly in low- and middle-income countries (LMICs), where limited resources worsen the impact of diarrheal diseases [9–12]. In Colombia, access to safe drinking water remains limited, affecting both rural and urban communities. Many rely on wells, ponds, and streams, which contribute to high rates of acute diarrheal diseases (ADDs), a leading cause of infant death. In 2024, 152 probable child deaths under five were reported, with 106 confirmed [13]. To address these issues, Colombia employs traditional microbiological detection methods such as membrane filtration and enzyme-based techniques focusing on *E. coli* and total coliforms [14,15]. While these methods are affordable and reliable, they take 18–48 h for results and cannot detect viable but non-culturable cells [16,17].

Recent technological advances have introduced faster, more sensitive options, such as PCR, genomic sequencing, mass spectrometry, and immunological tests [18,19]. However, these methods have limitations: PCR cannot distinguish between live and dead cells, requires specialized equipment, and trained personnel [20,21]. Immunological techniques also face challenges such as cross-reactivity among similar bacterial strains [19]. In this context, aptamers have emerged as promising tools for detection. These short DNA or RNA sequences form specific three-dimensional structures, allowing high-affinity and high-specificity binding to various molecular targets [22–24]. Created through SELEX, aptamers offer several advantages over antibodies, including lower production costs, greater stability, and the ability to bind to intracellular or hard-to-reach targets [25–28]. Coupling aptamers with magnetic nanoparticles (MNPs) further enhances analytical performance by enabling rapid and efficient separation of analytes, increasing sensitivity, and reducing interference [29,30]. This combination has expanded usage in microbiological detection, medical diagnostics, food safety, and environmental monitoring [31–39]. Although aptamer–MNP strategies for detecting *E. coli* have been explored, this study focuses on developing aptamers targeting a local environmental isolate from regional water sources. Environmental strains often differ genetically and phenotypically from reference strains, necessitating tailored detection tools. Therefore, the main goal of this research is to develop aptamers conjugated with MNPs that can detect an *E. coli* strain isolated from environmental water samples.

2. Materials and Methods

2.1. Bacterial Isolation

A water sample (~420 mL) was collected from a natural stream located at these coordinates: 6°09′29″ N 75°36′16″ W. The sample was obtained using a Schott glass bottle (500 mL capacity), ensuring a sampling depth of 7 cm and leaving an air chamber to maintain the viability of aerobic microorganisms. The sample was then filtered with a 0.45 µm filter and plated on nutrient media. The different colonies obtained were then isolated to obtain a pure culture.

2.2. Confirmation of Isolated Bacteria

Bacterial isolates were identified using the VITEK 2 COMPACT automated system (bioMérieux Industry, Marcy-l'Étoile, France), using Gram-negative cards as appropriate.

Both the equipment and the required reagents were provided by the Institución Universitaria Colegio Mayor de Antioquia (IUCMA).

2.3. Bacterial Culture

For preservation, the bacteria were inoculated into BHI broth and subsequently subcultured on blood agar (Columbia base). For the SELEX strategy, *E. coli* was used for positive selection and *A. baumannii* (NS1) was used for counter-selection; both were inoculated into BHI broth and incubated at 37 °C with agitation at 150 rpm overnight.

2.4. Cell-SELEX

We performed the Cell-SELEX strategy using the protocol published by Ospina et al. [40]. An ssDNA library of 78 nucleotides, with a variable region (N) of 40 nucleotides and two conserved regions (5′-TGACACCGTACCTGCTCT-40N-AAGCACGCCAGGGACT AT-3′) at the ends, was used to facilitate detection and amplification. This library was flanked by a forward oligonucleotide complementary to the 5′ conserved region (5′-TGACACCGTACCTGCTCT-3′) and a reverse oligonucleotide complementary to the 3′ conserved region (5′-ATAGTCCCTGGCGTGCTT-3′). The oligonucleotides and the library were synthesized by the company Macrogen, Rockville, MD, USA. We performed a counter-selection round against 100 µL of an overnight culture of the NS1 strain. For this, 1000 ng of the library, diluted in 100 µL of binding SELEX buffer (PBS 1X, 5 mM $MgCl_2$, and BSA (1 mg/mL), pH 7.4 in milliQ water), was heated to 95 °C for 10 min and cooled at room temperature to promote 3D folding. After 30 min of interaction with NS1 bacteria, the unbound molecules (NBMs) were recovered, and 5 µL was used for PCR amplification according to the protocol described below amplification profile: 95 °C for 2 min, then 95 °C for 30 s, 61 °C for 30 s, 72 °C for 30 s and a final step of 72 °C for 2 min for 20 cycles. For the first positive selection round (PS1), we used 100 µL of *E. coli* cultured in BHI medium. This was incubated with 10 µL of the PCR product from the negative round in 90 µL of binding SELEX buffer for 30 min at 27 °C and 50 rpm to promote interaction between ssDNA and *E. coli* surface targets and *E. coli* surface targets. The unbound molecules were separated by centrifugation at 8000 rpm, and bound ssDNA molecules were eluted with 100 µL of Milli-Q water at 95 °C for 5 min. Then, bound molecules (BMs) were amplified by PCR according to the previously described PCR protocol. Six positive selection (PS) rounds were performed to isolate the molecules capable of recognizing the *E. coli* bacteria from the previously obtained environmental isolate. The final PCR products were sent for identification by next-generation sequencing (NGS) at Admera Health (South Plainfield, NJ, USA) using the Illumina 2 × 250 platform (San Diego, CA, USA). In the PS rounds, the incubation time and the amount of *E. coli* culture used were gradually reduced. This was done to increase the detection capacity of the aptamers in the shortest possible time.

2.5. Next-Generation Sequencing (NGS) and Analysis

DNA libraries were prepared using the KAPA Hyper Prep PCR-free kit (Roche, Basel, Switzerland) for amplicon sequencing. Sample quality was assessed by Qubit and capillary electrophoresis, and libraries were quantified by qPCR. The sequencing was performed on an Illumina platform with 2 × 250 bp paired-end reads. The resulting fastq.gz files were processed with FAST QC software v0.12.1 [41] to determine the quality of the selected sequences. Subsequently, we used a custom Python v3.13.2 script to identify: (i) the total number of sequences obtained; (ii) sequences containing Illumina adapters; and (iii) sequences with the 40-nucleotide random region (N40) flanked by the conserved library regions 5′-TGACACCGTACCTGCTCT. . .AAGCACGCCAGGGACTAT-3′. Sequences corresponding to the N40 region were extracted and analyzed using the AptaSuite software platform v0.9.8 [42–44]. We performed analyses including enrichment profiling, aptamer

family composition, identification of representative secondary structures, clustering (via AptaCluster), and motif discovery [45,46].

2.6. Modular Aptamer Design

The top 10 motifs identified were aligned in Clustal W [47], and the common sequences were selected to design modular aptamers. These were incorporated into short sequences (<35 nucleotides) using artificial structural elements such as stems (e.g., 5′-GCAGC-[motif]-GCTGC-3′) or linker sequences. Designs were optimized to ensure (i) both motifs remain exposed and accessible for target recognition, (ii) the predicted secondary structure was stable (i.e., negative ΔG), and (iii) shorter sequence length.

Structural predictions were performed using the RNAfold web server [48] configured for DNA, with temperature set at 27 °C (matching Cell-SELEX conditions) and a salt concentration of 1 M. Special attention was given to the structural exposure of motifs within loops or unpaired regions to favor specific target binding.

2.7. Aptamer Synthesis

The most representative aptamer, APT-EC-1, and the most optimally designed modular aptamer, APT-EC-MUT, were synthesized by Macrogen, Rockville, MD, USA.

2.8. Magnetic Nanoparticle (MNP) Synthesis and Functionalization

We conducted the synthesis of magnetic nanoparticles (MNPs) using a co-precipitation method in an alkaline solution using the publicly available protocols from Bomb.bio [49–51]. For this, we used $FeCl_2$ (Sigma®, Burlington, MA, USA) and $FeCl_3$ (Sigma®), ensuring that the solutions were previously degassed and heated to 80–85 °C. The reaction was carried out under normal conditions, yielding magnetite (Fe_3O_4) nanoparticles ranging from 5 to 20 nm in size. Then, we washed and stored them in deionized water. For their functionalization, we applied a radical polymerization of methacrylic acid (MAA) in an aqueous medium. We used sodium dodecyl sulfate (SDS) (Sigma®) as a stabilizing agent and potassium persulfate ($K_2S_2O_8$) (Sigma®) as an initiator. The reaction proceeded at 70 °C for 2 h. Subsequently, we purified the functionalized MNPs by magnetic separation and successive washes. Finally, we stored the carboxyl-coated product in deionized water at room temperature [51,52]. The characterization of the magnetic nanoparticles obtained is found in Supplementary Materials S2.

2.9. Pull-Down

100 µL of carboxyl-functionalized magnetic nanoparticles (MNP-COOH) (10 mg/mL) was aliquoted into a 1.5 mL sterile Eppendorf tube. The tube was then placed on a magnetic rack for 1 min to allow complete separation of the MNPs from the supernatant, which was carefully removed. Next, three washes were performed using the aptamer-nanoparticle binding buffer (10 mM Tris, 100 mM NaCl, 10 mM $CaCl_2$, pH 7.4). Subsequently, 100 µL of aptamers (20 ng/µL) was added; the aptamers had been previously heated to 90 °C for 5 min and then cooled at room temperature for 10 min. The mixture was incubated at 4 °C for 15 min. Then, aptamers and MNPs were incubated for 5 min at room temperature with constant agitation at 50 rpm to facilitate the formation of the MNP-APT complexes. Following incubation, the coupled MNPs were magnetically separated, and the supernatant was discarded to remove any unbound aptamer. Subsequently, 100 µL of the isolated *E. coli* bacterial sample (pure and serial dilutions 1:10, 1:100, 1:1000, and 1:10,000) and ATCC reference strains as controls, including *E. coli* (positive control) and *E. faecalis*, *S. aureus*, *K. pneumoniae*, and *S. Typhimurium* (negative controls), previously cultured in BHI medium, were added according to the experimental design. The mixtures were incubated for 5 min at room temperature with constant agitation at 50 rpm. After incubation, magnetic separation

was performed to remove the unbound supernatant, followed by three washes (500 µL) with injectable water to eliminate non-specifically captured cells. Finally, the MNP–Aptamer complex retaining the bound bacteria was resuspended in 100 µL of sterile water; 10 µL was then plated on the selective medium for Gram-negative bacteria, MacConkey agar, and incubated for 24 h at 37 °C. The number of colonies on the agar was counted to calculate the total number of viable bacteria in the samples, and the specificity of the aptamer against *E. coli* was verified.

In addition, we performed an in situ assay with a new environmental water sample to verify the aptamers' ability to detect *E. coli* isolates. For this assay, the same protocol described above was followed, but at the sampling site under sterile conditions. The isolated bacteria were subsequently cultured in the laboratory to verify their quantity and specificity on MacConkey agar.

3. Results

3.1. Bacterial Isolation

The initial microorganisms isolated from blood agar showed whitish, opaque, and shiny colonies with convex elevations measuring 2–4 mm in the case of strain 1. Strain 2 showed shiny, colorless, nonhemolytic, smooth, and small colonies, 1–2 mm in size. In Gram staining, both strains were Gram-negative with a bacillary form for strain 1 and a coccobacillary form for strain 2 (Figure 1).

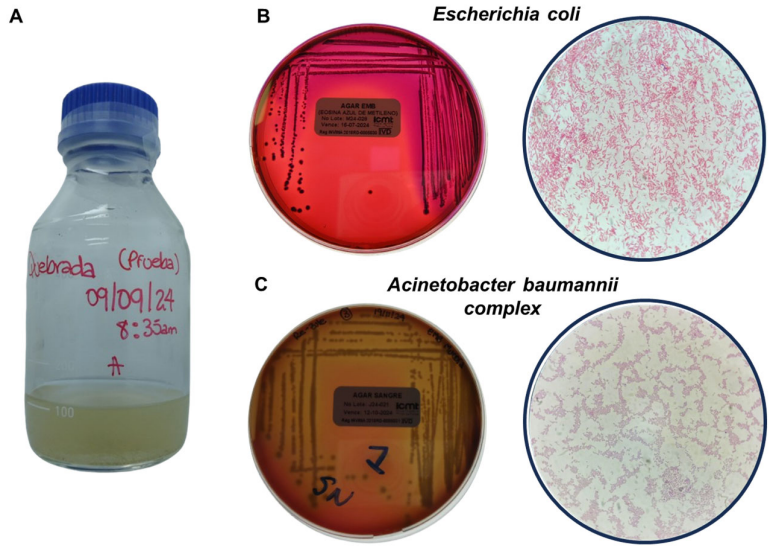

Figure 1. Isolated microorganisms from water sources: (**A**) Water sample collected from a natural water source. (**B**) *E. coli* strain isolated from the environmental water source, cultured on EMB agar, and Gram-stained, showing Gram-negative bacilli. (**C**) *A. baumannii* strain isolated from the environmental water source, cultured on blood agar, and Gram-stained, showing Gram-negative coccobacilli.

3.2. Confirmation of Isolated Bacteria

Strain 1 was identified as *E. coli* with a high level of confidence, which was the target microorganism for this study. Additionally, strain 2 was identified as *Acinetobacter baumannii* with a high level of confidence, which was used as a target for counter-selection in Cell-SELEX (Table 1). The original reports obtained by VITEK equipment can be found in Supplementary Materials S2.

Table 1. Results of the VITEK examination report.

Identified Organism	Probability	Confidence Level
Escherichia coli	96%	Excellent identification
Acinetobacter baumannii complex	99%	Excellent identification

3.3. Cell-SELEX

The Cell-SELEX strategy that allowed for the selection of ssDNA sequences with high affinity and specificity to *E. coli* is shown below in Figure 2.

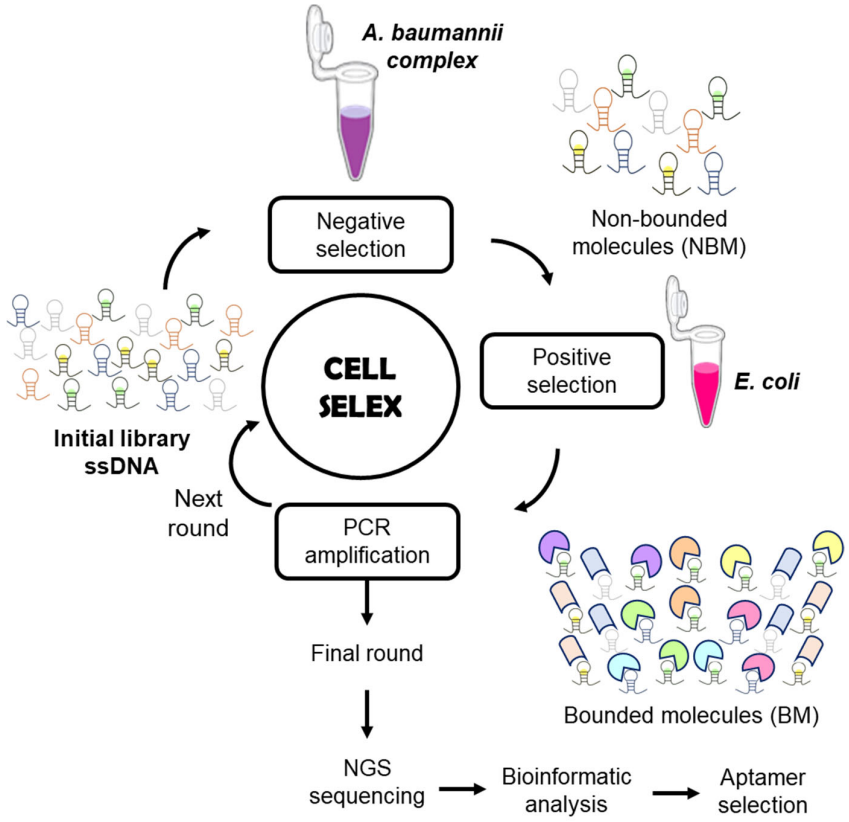

Figure 2. Illustration of the Cell-SELEX strategy employed in this study. NBM: non-bound molecules. BM: bound molecules.

DNA quantification in each round initially showed an increase in the recovery of bound molecules, followed by a progressive decrease in later rounds, indicating an improvement in the specificity of the selected aptamers (Figure 3A). As the process advanced, the reduction in incubation time and the amount of *E. coli* used facilitated the elimination of non-specific sequences, allowing for the selection of those with higher affinity (Figure 3B).

Electrophoresis analysis in agarose gel at 2% confirmed the amplification of PCR products in each round, as defined bands were observed in the positive selection rounds, while no amplification was detected in the negative controls, thereby ruling out contamination or non-specific amplification (Figure 3C).

In Table 2, we describe the detailed experimental design of the Cell-SELEX process employed in this study for the selection of specific aptamers against isolated *E. coli.* It presents the selection rounds, bacterial culture volumes used at each stage, the target bacterial species, and the incubation times applied. Throughout the process, these conditions were progressively adjusted to enhance selective pressure and promote the enrichment of sequences with greater specificity. The reduction in culture volume and incubation time

facilitated the elimination of low-affinity sequences, thereby optimizing the efficiency of aptamer selection for *E. coli.*

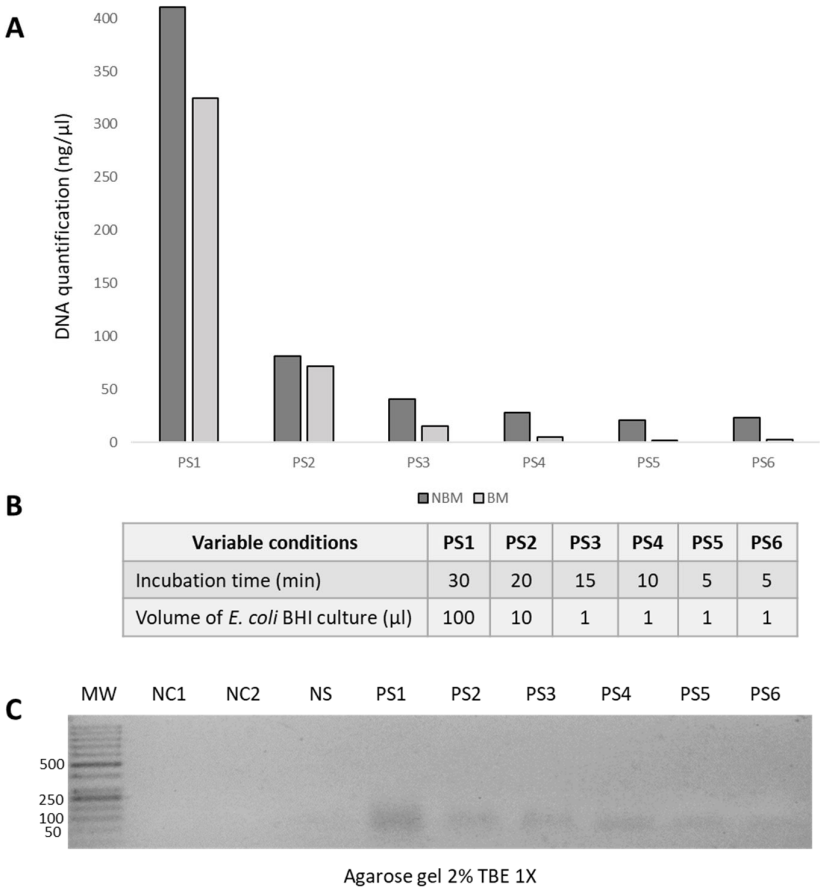

Variable conditions	PS1	PS2	PS3	PS4	PS5	PS6
Incubation time (min)	30	20	15	10	5	5
Volume of *E. coli* BHI culture (µl)	100	10	1	1	1	1

Figure 3. (**A**) Cell-SELEX Monitoring. (**A**) Quantification of DNA molecules obtained after each round of selection using NanoDrop (Thermo Fisher Scientific, Waltham, MA, USA). Quantification was performed once per round; no replicates were conducted; thus, error bars are not applicable. (**B**) Variable conditions were implemented throughout the Cell-SELEX strategy to improve aptamer specificity. (**C**) Electrophoresis of PCR products obtained after each Cell-SELEX round of selection. MW: molecular weight, NC1: negative control 1 without DNA, NC2: without oligonucleotides, NS: negative selection round, PS: positive selection rounds 1, 2, 3, 4, 5, and 6.

Table 2. Summary of Cell-SELEX rounds' design.

Round	Bacteria Specie	Bacteria Culture Volume (µL)	Incubation Time (min)	Type of Round
1	*A. baumannii*	100	30	Negative
2	*E. coli*	100	30	Positive
3	*E. coli*	10	20	Positive
4	*E. coli*	1	15	Positive
5	*E. coli*	1	10	Positive
6	*E. coli*	1	5	Positive
7	*E. coli*	1	5	Positive

3.4. Next-Generation Sequencing (NGS) and Analysis

A total of 508,256 sequences were obtained; 438,980 contained Illumina adapters, and 191,707 contained N40 regions within the conserved regions of the initial library. Approximately 12% of sequences showed enrichment. The percentage of base distribution was as follows: A: 17.6%, C: 22.3%, G: 31.1%, and T: 28.9%, compared to the initial library's A: 26%, C: 26.7%, G: 24.5%, and T: 22.6%. The aptamer candidates' ID, sequences, count,

and frequencies are shown in Figure 4A. The 2D structure of the most representative aptamer is shown in Figure 4B; the alignment of the 10 most frequent motifs is observed in Figure 4C; and the 2D structure of the modular aptamer designed based on the motifs found is observed in Figure 4D.

A

Id	Randomized Region	Round no.6, final	
		Count	Frequency
17580	GTGGAGGCGCTCCGTTGCACAGATTTAGTGATGTCTGCCC	36.549	3.65E-5
78527	TTTTCTCCATAACCACGTCGCCCAGATAATGCGCGGTTGG	31.328	3.13E-5
100079	GCTTCGGCCCTCTTGGCGGTTGGTCCAGGTGGGGTTTGGG	31.328	3.13E-5
13915	CGCATCCGTGCAACGGAATCTGTATTCCACGCGTCCGTCG	31.328	3.13E-5
93903	CGGGGAAGCGGGGCACGTGGCCTTCGGGGGATCCAGCGGC	31.328	3.13E-5
128798	AGGGAAAGTCGTTCTTCTGGGCGTTCGTACTCTGGACGGT	31.328	3.13E-5
124271	CGGGGGTAAACACTAAAACACATAATCTGTGACAGAAGGC	26.107	2.61E-5
158874	GGCAGAGTACCCAAACAAGCAAAAACGCAAGACTCGTCCC	26.107	2.61E-5
75219	CGGATTCTGTTGTGTGATTGTTGTTTATGCTATTTGATGG	26.107	2.61E-5
36645	AGTTTTCTGACTTTGCTTTGGGCTCCCCTGTTAATTATTC	26.107	2.61E-5

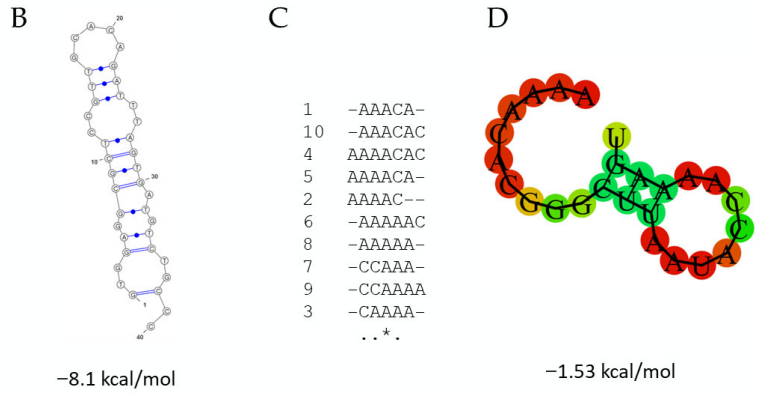

Figure 4. Aptamers selected through bioinformatics tools after NGS sequencing: (**A**) Top 10 aptamers obtained. (**B**) 2D structure of the top 1 aptamer. (**C**) Top 10 motif discovery alignment. (**D**) Design of a modular aptamer.

3.5. Pull-Down

The summary of the pull-down strategy carried out is described in Figure 5. The specificity of both aptamers was evaluated by monitoring bacterial growth in the presence of *Escherichia coli*. The bacterial strains and isolates used for this laboratory-scale validation are detailed in Figure 6A. The results obtained using the EC aptamer are shown in the upper and lower panels of Figure 6B, while those corresponding to the modular aptamer EC_MUT are shown in the upper and lower panels of Figure 6C.

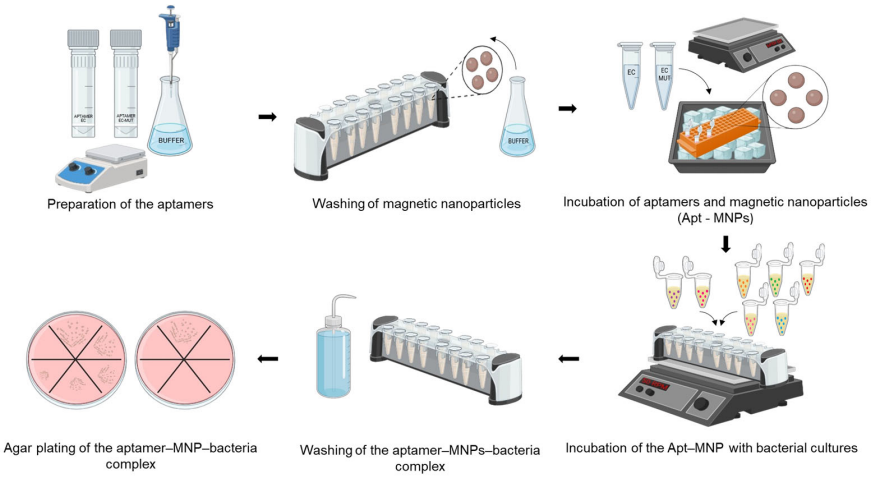

Figure 5. Pull-down strategy for aptamer validation under controlled laboratory conditions using isolated and ATCC reference strains.

A

Microorganisms	
1. *E. coli* pure	**7.** *E. coli* ATCC pure
2. *E. coli* 1:10	**8.** *E. faecalis* ATCC pure
3. *E. coli* 1:100	**9.** *S. Typhymurium* ATCC pure
4. *E. coli* 1:1000	**10.** *K. pneumoniae* ATCC pure
5. *E. coli* 1:10000	**11.** *S. aureus* ATCC pure
6. MNPs	**12.** *A. baumannii* pure

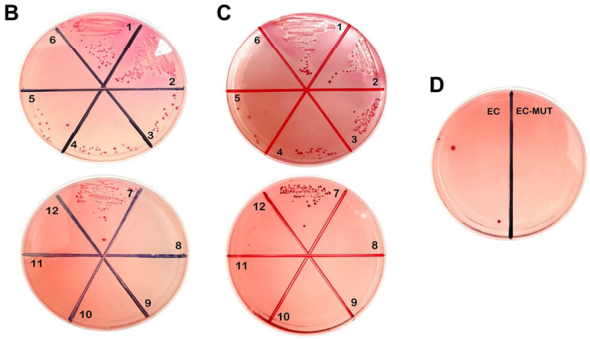

E

Number of colonies obtained	EC	EC-MUT
1	TNTC	TNTC
2	TNTC	TNTC
3	16	64
4	20	21
5	15	6
6	0	0
7	TNTC	TNTC
8	0	0
9	0	0
10	0	0
11	0	0
12	0	3
In-situ	3	0

Figure 6. Pull-down assay results for *E. coli* detection using aptamers: (**A**) Microbial strains and concentrations used in the pull-down assay. (**B**) Results obtained using the EC aptamer. (**C**) Results obtained using the modular aptamer EC-MUT. (**D**) Results obtained using the EC and EC-MUT aptamers in a preliminary in situ test with a new environmental water sample. (**E**) Quantification of the number of *E. coli* colonies obtained under each experimental condition using EC aptamer and EC-MUT aptamer. Data represent the absolute colony counts observed after magnetic separation, showing the relative efficiency of each aptamer in bacterial isolation. TNTC: too numerous to count.

In both cases, bacterial growth was observed with the pure *E. coli* environmental isolate and across all tested dilutions (1:10, 1:100, 1:1000, and 1:10,000), as well as with the pure *E. coli* ATCC reference strain. No growth was detected when magnetic nanoparticles without aptamers were used, nor with any of the other tested ATCC Enterobacteriaceae strains. These results demonstrate that both aptamers selectively bind to *E. coli* and do not exhibit non-specific interactions with non-target bacterial species under the experimental conditions applied.

4. Discussion

The detection of microorganisms has long been essential in fields such as public health, biotechnology, and environmental microbiology. In recent years, aptamers have emerged as a promising alternative for microbial detection due to their high specificity and adaptability. This study employed the Cell-SELEX technique to isolate aptamers targeting *Escherichia coli*, a key fecal contamination indicator. By using an environmental isolate, the selection strategy was designed to closely reflect real-world application scenarios.

Selective pressure progressively increased throughout the Cell-SELEX rounds to enhance specificity, which enabled the identification of high-affinity candidates in fewer cycles than traditionally reported [53,54]. A single counter-selection round was incorporated early to reduce non-specific binding, balancing sensitivity and specificity [55,56].

Next-generation sequencing (NGS) of the sixth positive round generated a complex dataset, which was refined using a custom Python pipeline to remove adapters, conserved regions, and short sequences. Structural predictions via RNAfold revealed common aptamer motifs, such as stem-loops, which facilitate specific target binding [54,57,58]. These conformations are critical for molecular recognition and are consistent with previous structural models describing aptamer–target interaction as a "molecular embrace" [57,59–65].

Candidate selection considered thermodynamic stability (ΔG), with top sequences showing values from 0.0 to −14.7 kcal/mol, aligning with commonly accepted functional

ranges [66–69]. A representative aptamer and a modular version (under 40 nt) were synthesized, the latter designed to retain key binding motifs while minimizing synthesis costs, in line with recent trends toward truncated aptamer development [26,70–74].

Although chemical modifications were not implemented, the potential for enhanced stability through backbone alterations, end-capping, or locked nucleic acids remains relevant for future integration [28,75–79]. Aptamers were conjugated onto magnetic nanoparticles (MNPs) functionalized with carboxyl groups (-COOH), chosen for their favorable handling, stability, and cost-effectiveness (Table S1). MNPs allowed for rapid magnetic separation, eliminating the need for biotinylation while maintaining performance [80,81].

The carboxyl-functionalized nanoparticles were obtained following the BOMB.bio protocol. The surface of these MNPs allows aptamer binding through electrostatic interactions, which were optimized by carefully controlling the pH, buffer composition, and short incubation times. These parameters were deliberately designed during the SELEX strategy development to ensure rapid and stable formation of aptamer–MNP complexes, enabling efficient pull-down of the *E. coli* target.

In this study, the incubation time between the aptamer-functionalized magnetic nanoparticles (MNPs) and *E. coli* was set to 5 min. This parameter was also optimized during the SELEX process, where interaction times were progressively reduced from 30 min in the initial rounds to 5 min in rounds six and seven, favoring the selection of aptamers capable of rapid binding. While the literature on aptamer–bacteria binding kinetics remains limited, several studies have demonstrated that aptamer–target interactions can occur within short timescales. For instance, fluorescence-based kinetic studies have reported equilibrium binding within 5–10 min for thrombin-specific aptamers [82]. Similarly, recent work on aptamer–protein recognition confirmed association times under 5 min when using optimized conditions [83]. These findings support the feasibility of short incubation times in aptamer-based systems, which is particularly advantageous for the development of rapid, field-deployable detection platforms.

In vitro, assays demonstrated that both the full-length EC aptamer and the modular variant were able to successfully recognize the environmental *E. coli* isolate as well as the *E. coli* ATCC reference strain, detecting both in their pure form and across serial dilutions down to 1:10,000. For the initial in situ validation, a second water sample was collected. Unlike the first (turbid) sample, this one appeared clear and nearly transparent, likely due to environmental factors at the time of collection. Under these conditions, the EC aptamer successfully detected three *E. coli* colonies, while the modular aptamer failed to detect any. This discrepancy may be attributed to a low bacterial load in the sample and the still-uncertain mechanisms governing aptamer–bacteria interactions. These findings highlight the need for additional validation studies under diverse environmental conditions to better understand aptamer performance and binding dynamics in real-world applications.

Overall, this detection strategy represents a promising step toward aptamer-based biosensing for *E. coli*. Future work should focus on integrating colorimetric or electrochemical detection systems to enable rapid, accessible readouts. Approaches such as sandwich-type assays with gold nanoparticles [36] or phenol red-based indicators leveraging urease activity [84,85] offer practical pathways toward real-world deployment.

5. Conclusions

The results of this study highlight the potential of aptamers as highly specific molecular recognition elements for the detection of *Escherichia coli*, supporting their application in water quality monitoring. The aptamer–magnetic nanoparticle (MNP) system developed here represents a significant step toward the creation of a rapid, cost-effective, and portable biosensor, particularly suited for use in low-resource settings. Although the functionality

of the aptamer–MNP complex was validated in vitro through culture-based assays, further optimization is required to enable direct, faster detection without the need for culturing. It should be noted that in this study, we did not assess the ability of the selected aptamers to distinguish between viable and non-viable *Escherichia coli* cells, since culture-based confirmation was used. Future work will include additional experiments using UV-inactivated or otherwise treated bacteria to evaluate aptamer performance with live versus dead cells, which will be essential for the development of a fully reliable detection platform. Preliminary in situ testing also revealed performance differences between the full-length and modular aptamers, emphasizing the need for robust validation under diverse environmental conditions. Future efforts should focus on integrating efficient signal transduction mechanisms, such as colorimetric or electrochemical outputs, to advance toward a fully field-deployable diagnostic platform for real-time microbial monitoring.

Supplementary Materials: The following supporting information can be downloaded at: https://www.mdpi.com/article/10.3390/environments12090329/s1, Table S1: Comparison of current methods vs. the proposed method for Environmental *E. coli* isolation; Supplementary Material S2. Morphological and surface analysis by field emission scanning electron microscopy (FESEM), and Elemental identification using an X-ray probe. The references [86–91] were cited in the Supplementary Materials.

Author Contributions: Conceptualization, J.D.O.-V. and M.M.S.-J.; methodology, J.D.O.-V. and M.M.S.-J.; software, J.D.O.-V.; validation, Z.H.-R.; formal analysis, J.D.O.-V. and M.M.S.-J.; investigation, Z.H.-R., W.Y.R.-B. and M.O.P.-N.; resources, J.D.O.-V.; data curation, J.D.O.-V. and Z.H.-R.; writing—original draft preparation, J.D.O.-V., Z.H.-R. and M.M.S.-J.; writing—review and editing, J.D.O.-V., Z.H.-R. and M.M.S.-J.; supervision, J.D.O.-V.; project administration, J.D.O.-V.; funding acquisition, J.D.O.-V. All authors have read and agreed to the published version of the manuscript.

Funding: This research received no external funding.

Data Availability Statement: The data generated in this project are available in the Supplementary Information.

Acknowledgments: We used ChatGPT 4.5 to improve the clarity, fluency, and grammatical accuracy of the English language. The core scientific content, data analysis, interpretation of results, and original writing were entirely conducted by the authors. All outputs generated with AI were carefully reviewed, edited, and approved by the authors to ensure accuracy and adherence to the scientific integrity of the manuscript.

Conflicts of Interest: The authors declare no conflicts of interest.

Abbreviations

The following abbreviations are used in this manuscript:

E. coli	*Escherichia coli*
SDG	Sustainable Development Goals
JMP	Joint Monitoring Programme for Water Supply, Sanitation, and Hygiene
WHO	World Health Organization
UNICEF	United Nations Children's Fund
LMICs	Low- and middle-income countries
ADDs	Acute diarrheal diseases
DNA	Deoxyribonucleic acid
RNA	Ribonucleic acid
PCR	Polymerase chain reaction
Apt	Aptamer
SELEX	Systematic evolution of ligands by exponential enrichment
MNPs	Magnetic nanoparticles
BM	Bound molecules

NBM	Unbound molecules
PS	Positive selection
NS	Negative selection
NGS	Next-generation sequencing
MAA	Methacrylic acid
SDS	Sodium dodecyl sulfate
AuNP	Gold nanoparticle
µL	Microliters
mL	Millilitre
cm	Centimetre
µm	Micrometre
mg	Milligrams
ng	Nanogram
rpm	Revolutions per minute
IUCMA	Institución Universitaria Colegio Mayor de Antioquia

References

1. UNDP. Goal 6: Clean Water and Sanitation | Sustainable Development Goals | United Nations Development Programme. Available online: https://www.undp.org/sustainable-development-goals/clean-water-and-sanitation (accessed on 30 May 2025).
2. WHO/UNICEF Joint Monitoring Program for Water Supply, Sanitation and Hygiene (JMP)—Progress on Household Drinking Water, Sanitation, and Hygiene 2000–2022: Special Focus on Gender. Available online: https://www.unwater.org/publications/who/unicef-joint-monitoring-program-update-report-2023 (accessed on 30 May 2025).
3. Lin, L.; Yang, H.; Xu, X. Effects of water pollution on human health and disease heterogeneity: A review. *Front. Environ. Sci.* **2022**, *10*, 880246. Available online: https://www.frontiersin.org/journals/environmental-science/articles/10.3389/fenvs.2022.880246/full (accessed on 30 May 2025). [CrossRef]
4. Qadri, R.; Faiq, M.A. Freshwater pollution: Effects on aquatic life and human health. In *Freshwater Pollution: Dynamics and Remediation*; Qadri, H., Bhat, R.A., Mehmood, M.A., Dar, G.H., Eds.; Springer: Singapore, 2020; pp. 15–26. [CrossRef]
5. Magana-Arachchi, D.N.; Wanigatunge, R.P. Ubiquitous waterborne pathogens. In *Waterborne Pathogens: Detection and Treatment*; Vara Prasad, M.N., Grobelak, A., Eds.; Butterworth-Heinemann: Oxford, UK, 2020; pp. 15–42. Available online: https://www.sciencedirect.com/science/article/pii/B9780128187838000025 (accessed on 15 June 2025).
6. Alegbeleye, O.O.; Sant'Ana, A.S. Manure-borne pathogens as an important source of water contamination: An update on the dynamics of pathogen survival/transport as well as practical risk mitigation strategies. *Int. J. Hyg. Environ. Health* **2020**, *227*, 113524. Available online: https://www.sciencedirect.com/science/article/pii/S1438463920300262 (accessed on 15 June 2025). [CrossRef] [PubMed]
7. Li, E.; Saleem, F.; Edge, T.A.; Schellhorn, H.E. Biological indicators for fecal pollution detection and source tracking: A review. *Processes* **2021**, *9*, 2058. [CrossRef]
8. Some, S.; Mondal, R.; Mitra, D.; Jain, D.; Verma, D.; Das, S. Microbial pollution of water with special reference to coliform bacteria and their nexus with environment. *Energy Nexus* **2021**, *1*, 100008. Available online: https://www.sciencedirect.com/science/article/pii/S2772427121000085 (accessed on 17 June 2025). [CrossRef]
9. Khan, F.M.; Gupta, R. Escherichia coli (*E. coli*) as an indicator of fecal contamination in groundwater: A review. In *Sustainable Development of Water and Environment: Proceedings of the ICSDWE2020, Incheon, Republic of Korea, 13–14 January 2020*; Jeon, H.Y., Ed.; Springer International Publishing: Cham, Switzerland, 2020; pp. 225–235.
10. Odonkor, S.T.; Mahami, T. *Escherichia coli* as a tool for disease risk assessment of drinking water sources. *Int. J. Microbiol.* **2020**, *2020*, 8472. Available online: https://onlinelibrary.wiley.com/doi/abs/10.1155/2020/2534130 (accessed on 15 June 2025). [CrossRef]
11. Hernández-Vásquez, A.; Visconti-Lopez, F.J.; Vargas-Fernández, R. *Escherichia coli* contamination of water for human consumption and its associated factors in Peru: A cross-sectional study. *Am. J. Trop. Med. Hyg.* **2022**, *108*, 187–194. Available online: https://pmc.ncbi.nlm.nih.gov/articles/PMC9833058/ (accessed on 30 May 2025).
12. Camacho-Botero, L.A. La paradoja de la disponibilidad de agua de mala calidad en el sector rural colombiano. *Rev. Ing.* **2020**, *1*, 38–51. Available online: https://revistas.uniandes.edu.co/index.php/rdi/article/view/7489 (accessed on 15 June 2025). [CrossRef]
13. Instituto Nacional de Salud Colombia. Boletín Epidemiológico Semanal; Vigilancia Intensificada de Lesiones por Pólvora Pirotécnica; Semana Epidemiológica 52 (Dic 22-28, 2024). Available online: https://www.ins.gov.co/BibliotecaDigital/2024-boletin-epidemiologico-semana-52.pdf (accessed on 18 May 2025).

14. Informe Nacional de Calidad del Agua para Consumo Humano. 2025. Available online: https://www.minvivienda.gov.co/taxonomy/term/1813 (accessed on 2 September 2025).
15. Ministerio de la Protección Social Colombia. Resolución 1618 de 2010 Por la Cual se Reglamenta Parcialmente el Decreto 2171 de 2009. Available online: https://www.alcaldiabogota.gov.co/sisjur/normas/Norma1.jsp?i=39524 (accessed on 15 May 2025).
16. McConn, B.R.; Kraft, A.L.; Durso, L.M.; Ibekwe, A.M.; Frye, J.G.; Wells, J.E.; Tobey, E.M.; Ritchie, S.; Williams, C.F.; Cook, K.L.; et al. An analysis of culture-based methods used for the detection and isolation of *Salmonella* spp., *Escherichia coli*, and *Enterococcus* spp. from surface water: A systematic review. *Sci. Total Environ.* **2024**, *927*, 172–190. Available online: https://www.sciencedirect.com/science/article/pii/S0048969724023337 (accessed on 23 May 2025). [CrossRef]
17. Saleem, F.; Edge, T.A.; Schellhorn, H.E. Validation of qPCR method for enterococci quantification at Toronto beaches: Application for rapid recreational water monitoring. *J. Gt. Lakes Res.* **2022**, *48*, 707–716. Available online: https://www.sciencedirect.com/science/article/pii/S0380133022000466 (accessed on 13 June 2025). [CrossRef]
18. Ezenarro, J.J.; Mas, J.; Muñoz-Berbel, X.; Uria, N. Advances in bacterial concentration methods and their integration in portable detection platforms: A review. *Anal. Chim. Acta* **2022**, *1209*, 339079. Available online: https://www.sciencedirect.com/science/article/pii/S0003267021009053 (accessed on 15 June 2025). [CrossRef]
19. Tambi, A.; Brighu, U.; Gupta, A.B. Methods for detection and enumeration of coliforms in drinking water: A review. *Water Supply* **2023**, *23*, 4047–4058. [CrossRef]
20. Takci, H.A.M.; Karaca, C. A comparison study of quantitative PCR and conventional culture-based methods for microbial water quality. *Res. Sq.* **2022**. Available online: https://www.researchsquare.com/article/rs-1497117/v1 (accessed on 10 June 2025).
21. Heijnen, L.; de Vries, H.J.; van Pelt, G.; Stroobach, E.; Atsma, A.; Vranken, J.; De Maeyer, K.; Vissers, L.; Medema, G. Qualitative detection of *E. coli* in distributed drinking water using real-time reverse transcription PCR targeting 16S rRNA: Validation and practical experiences. *Water Res.* **2024**, *259*, 121843. Available online: https://www.sciencedirect.com/science/article/pii/S0043135424007449 (accessed on 13 June 2025). [CrossRef]
22. Ellington, A.D.; Szostak, J.W. In vitro selection of RNA molecules that bind specific ligands. *Nature* **1990**, *346*, 818–822. Available online: https://www.nature.com/articles/346818a0 (accessed on 15 February 2025). [CrossRef]
23. Tuerk, C.; Gold, L. Systematic Evolution of Ligands by Exponential Enrichment: RNA ligands to bacteriophage T4 DNA polymerase. *Science* **1990**, *249*, 505–510. Available online: https://www.science.org/doi/abs/10.1126/science.2200121 (accessed on 15 February 2025). [CrossRef]
24. Robertson, D.L.; Joyce, G.F. Selection in vitro of an RNA enzyme that specifically cleaves single-stranded DNA. *Nature* **1990**, *344*, 467–468. Available online: https://www.nature.com/articles/344467a0 (accessed on 15 February 2025). [CrossRef]
25. Hao, L.; Gu, H. Introduction of aptamer, SELEX, and different SELEX variants. In *Aptamers for Medical Applications: From Diagnosis to Therapeutics*; Dong, Y., Ed.; Springer: Singapore, 2021; pp. 1–30. [CrossRef]
26. Kohlberger, M.; Gadermaier, G. SELEX: Critical factors and optimization strategies for successful aptamer selection. *Biotechnol. Appl. Biochem.* **2021**, *69*, 1771–1792. [CrossRef]
27. Ștefan, G.; Hosu, O.; De Wael, K.; Lobo-Castañón, M.J.; Cristea, C. Aptamers in biomedicine: Selection strategies and recent advances. *Electrochim. Acta* **2021**, *376*, 137994. Available online: https://www.sciencedirect.com/science/article/pii/S001346862100284X (accessed on 15 February 2025). [CrossRef]
28. Domsicova, M.; Korcekova, J.; Poturnayova, A.; Breier, A. New insights into aptamers: An alternative to antibodies in the detection of molecular biomarkers. *Int. J. Mol. Sci.* **2024**, *25*, 6833. [CrossRef] [PubMed]
29. Gutiérrez-Santana, J.C.; Toscano-Garibay, J.D.; López-López, M.; Coria-Jiménez, V.R. Aptamers coupled to nanoparticles in the diagnosis and treatment of microbial infections. *Enfermedades Infecc. Microbiol. Clin. Engl. Ed.* **2020**, *38*, 331–337. Available online: https://www.sciencedirect.com/science/article/pii/S2529993X20301222 (accessed on 13 June 2025). [CrossRef]
30. Uğurlu, Ö.; Man, E.; Gök, O.; Ülker, G.; Soytürk, H.; Özyurt, C.; Evran, S. A review of aptamer-conjugated nanomaterials for analytical sample preparation: Classification according to the utilized nanomaterials. *Anal. Chim. Acta* **2024**, *1287*, 342001. Available online: https://www.sciencedirect.com/science/article/pii/S0003267023012229 (accessed on 15 June 2025). [CrossRef]
31. Xu, R.; Ouyang, L.; Chen, H.; Zhang, G.; Zhe, J. Recent advances in biomolecular detection based on aptamers and nanoparticles. *Biosensors* **2023**, *13*, 474. [CrossRef]
32. Clack, K.; Sallam, M.; Muyldermans, S.; Sambasivam, P.; Nguyen, C.M.; Nguyen, N.T. Instant *Candida albicans* detection using ultra-stable aptamer-conjugated gold nanoparticles. *Micromachines* **2024**, *15*, 216. [CrossRef]
33. Sargazi, S.; Simge, E.R.; Mobashar, A.; Gelen, S.S.; Rahdar, A.; Ebrahimi, N.; Hosseinikhah, S.M.; Bilal, M.; Kyzas, G.Z. Aptamer-conjugated carbon-based nanomaterials for cancer and bacteria theranostics: A review. *Chem. Biol. Interact.* **2022**, *361*, 109964. Available online: https://www.sciencedirect.com/science/article/pii/S0009279722001697 (accessed on 20 May 2025). [CrossRef]
34. Dabhade, A.H.; Verma, R.P.; Paramasivan, B.; Kumawat, A.; Saha, B. Development of silver nanoparticles and aptamer-conjugated biosensor for rapid detection of *E. coli* in a water sample. *3 Biotech* **2023**, *13*, 244. [CrossRef]
35. Pandit, C.; Alajangi, H.K.; Singh, J.; Khajuria, A.; Sharma, A.; Hassan, M.S.; Parida, M.; Semwal, A.D.; Gopalan, N.; Sharma, R.K.; et al. Development of magnetic nanoparticle-assisted aptamer-quantum dot based biosensor for the detection of *Escherichia coli* in

water samples. *Sci. Total Environ.* **2022**, *831*, 154857. Available online: https://www.sciencedirect.com/science/article/pii/S0048969722019507 (accessed on 13 June 2025). [CrossRef] [PubMed]
36. Sadsri, V.; Trakulsujaritchok, T.; Tangwattanachuleeporn, M.; Hoven, V.P.; Na Nongkhai, P. Simple colorimetric assay for *Vibrio parahaemolyticus* detection using aptamer-functionalized nanoparticles. *ACS Omega* **2020**, *5*, 21437–21442. [CrossRef] [PubMed]
37. Gupta, R.; Kumar, A.; Kumar, S.; Pinnaka, A.K.; Singhal, N.K. Naked eye colorimetric detection of *Escherichia coli* using aptamer conjugated graphene oxide enclosed Gold nanoparticles. *Sens. Actuators B Chem.* **2021**, *329*, 129100. Available online: https://www.sciencedirect.com/science/article/pii/S0925400520314404 (accessed on 13 June 2025). [CrossRef]
38. Lim, S.H.; Ryu, Y.C.; Hwang, B.H. Aptamer-immobilized gold nanoparticles enable facile and on-site detection of *Staphylococcus aureus*. *Biotechnol. Bioprocess Eng.* **2021**, *26*, 107–113. [CrossRef]
39. Park, J.; Shin, E.; Yeom, J.H.; Choi, Y.; Joo, M.; Lee, M.; Kim, J.H.; Bae, J.; Lee, K. Gold nanoparticle-DNA aptamer-assisted delivery of antimicrobial peptide effectively inhibits *Acinetobacter baumannii* infection in mice. *J. Microbiol.* **2022**, *60*, 128–136. [CrossRef]
40. Ospina-Villa, J.D.; Restrepo-Cano, V.; Sánchez-Jiménez, M.M. Bio-SELEX: A strategy for biomarkers isolation directly from biological samples. *Methods Protoc.* **2023**, *6*, 109. [CrossRef]
41. Andrews, S. *FastQC: A Quality Control Tool for High Throughput Sequence Data*; Babraham Bioinformatics: Cambridge, UK, 2010. Available online: http://www.bioinformatics.babraham.ac.uk/projects/fastqc/ (accessed on 13 June 2025).
42. Hoinka, J.; Backofen, R.; Przytycka, T.M. AptaSUITE: A full-featured bioinformatics framework for the comprehensive analysis of aptamers from HT-SELEX experiments. *Mol. Ther.-Nucleic Acids.* **2018**, *11*, 515–517. Available online: https://www.sciencedirect.com/science/article/pii/S2162253118300507 (accessed on 12 July 2025). [CrossRef]
43. Hoinka, J.; Przytycka, T. AptaPLEX—A dedicated, multithreaded demultiplexer for HT-SELEX data. *Methods* **2016**, *106*, 82–85. Available online: https://www.sciencedirect.com/science/article/pii/S1046202316300834 (accessed on 15 July 2025). [CrossRef] [PubMed]
44. Hoinka, J.; Berezhnoy, A.; Dao, P.; Sauna, Z.E.; Gilboa, E.; Przytycka, T.M. Large scale analysis of the mutational landscape in HT-SELEX improves aptamer discovery. *Nucleic Acids Res.* **2015**, *43*, 5699–5707. [CrossRef] [PubMed]
45. Hoinka, J.; Berezhnoy, A.; Sauna, Z.E.; Gilboa, E.; Przytycka, T.M. AptaCluster—A method to cluster HT-SELEX aptamer pools and lessons from its application. *Res. Comput. Mol. Biol.* **2014**, *8394*, 115. Available online: https://pmc.ncbi.nlm.nih.gov/articles/PMC4281958/ (accessed on 13 July 2025).
46. Dao, P.; Hoinka, J.; Takahashi, M.; Zhou, J.; Ho, M.; Wang, Y.; Costa, F.; Rossi, J.J.; Backofen, R.; Burnett, J.; et al. AptaTRACE elucidates RNA Sequence-Structure motifs from selection trends in HT-SELEX experiments. *Cell Syst.* **2016**, *3*, 62–70. Available online: https://www.sciencedirect.com/science/article/pii/S2405471216302204 (accessed on 30 May 2025). [CrossRef] [PubMed]
47. Thompson, J.D.; Higgins, D.G.; Gibson, T.J. CLUSTAL W: Improving the sensitivity of progressive multiple sequence alignment through sequence weighting, position-specific gap penalties and weight matrix choice. *Nucleic Acids Res.* **1994**, *22*, 4673. Available online: https://pmc.ncbi.nlm.nih.gov/articles/PMC308517/ (accessed on 15 May 2025).
48. Lorenz, R.; Bernhart, S.H.; Höner zu Siederdissen, C.; Tafer, H.; Flamm, C.; Stadler, P.F.; Hofacker, I.L. ViennaRNA Package 2.0. *Algorithms Mol. Biol.* **2011**, *6*, 26. [CrossRef]
49. Wu, W.; Wu, Z.; Yu, T.; Jiang, C.; Kim, W.S. Recent progress on magnetic iron oxide nanoparticles: Synthesis, surface functional strategies, and biomedical applications. *Sci. Technol. Adv. Mater.* **2015**, *16*, 023501. [CrossRef]
50. Choi, J.; Kim, J.C.; Lee, Y.B.; Kim, I.S.; Park, Y.K.; Hur, N.H. Fabrication of silica-coated magnetic nanoparticles with highly photoluminescent lanthanide probes. *Chem. Commun.* **2007**, 1644–1646. [CrossRef]
51. Oberacker, P.; Stepper, P.; Bond, D.M.; Höhn, S.; Focken, J.; Meyer, V.; Schelle, L.; Sugrue, V.J.; Jeunen, G.J.; Moser, T.; et al. Bio-On-Magnetic-Beads (BOMB): Open platform for high-throughput nucleic acid manipulation. *PLoS Biol.* **2019**, *17*, e3000107. [CrossRef]
52. Yu, S.; Chow, G.M. Carboxyl group (–CO2H) functionalized ferrimagnetic iron oxide nanoparticles for potential bio-applications. *J. Mater. Chem.* **2004**, *14*, 2781–2786. Available online: https://pubs.rsc.org/en/content/articlelanding/2004/jm/b404964k (accessed on 15 June 2025). [CrossRef]
53. Marton, S.; Cleto, F.; Krieger, M.A.; Cardoso, J. Isolation of an aptamer that binds specifically to *E. coli*. *PLoS ONE* **2016**, *11*, e0153637. Available online: https://journals.plos.org/plosone/article?id=10.1371/journal.pone.0153637 (accessed on 15 June 2025). [CrossRef]
54. Yu, X.; Chen, F.; Wang, R.; Li, Y. Whole-bacterium SELEX of DNA aptamers for rapid detection of *E.coli* O157:H7 using a QCM sensor. *J. Biotechnol.* **2018**, *266*, 39–49. Available online: https://www.sciencedirect.com/science/article/pii/S0168165617317686 (accessed on 19 June 2025). [CrossRef]
55. Dwivedi, H.P.; Smiley, R.D.; Jaykus, L.A. Selection of DNA aptamers for capture and detection of *Salmonella* Typhimurium using a whole-cell SELEX approach in conjunction with cell sorting. *Appl. Microbiol. Biotechnol.* **2013**, *97*, 3677–3686. [CrossRef]
56. Suh, S.H.; Dwivedi, H.P.; Choi, S.J.; Jaykus, L.A. Selection and characterization of DNA aptamers specific for *Listeria* species. *Anal. Biochem.* **2014**, *459*, 39–45. Available online: https://www.sciencedirect.com/science/article/pii/S0003269714002097 (accessed on 15 June 2025). [CrossRef] [PubMed]

57. Kim, Y.S.; Song, M.Y.; Jurng, J.; Kim, B.C. Isolation and characterization of DNA aptamers against *Escherichia coli* using a bacterial cell–systematic evolution of ligands by exponential enrichment approach. *Anal. Biochem.* **2013**, *436*, 22–28. Available online: https://www.sciencedirect.com/science/article/pii/S0003269713000341 (accessed on 15 June 2025). [CrossRef] [PubMed]
58. Pleiko, K.; Saulite, L.; Parfejevs, V.; Miculis, K.; Vjaters, E.; Riekstina, U. Differential binding cell-SELEX method to identify cell-specific aptamers using high-throughput sequencing. *Sci. Rep.* **2019**, *9*, 8142. Available online: https://www.nature.com/articles/s41598-019-44654-w (accessed on 30 May 2025).
59. Siddiqui, S.; Yuan, J. Binding characteristics study of DNA based aptamers for *E. coli* O157:H7. *Molecules* **2021**, *26*, 204. [CrossRef]
60. Amraee, M.; Oloomi, M.; Yavari, A.; Bouzari, S. DNA aptamer identification and characterization for *E. coli* O157 detection using cell based SELEX method. *Anal. Biochem.* **2017**, *536*, 36–44. Available online: https://www.sciencedirect.com/science/article/pii/S0003269717303378 (accessed on 13 June 2025). [CrossRef]
61. Hermann, T.; Patel, D.J. Adaptive recognition by nucleic acid aptamers. *Science* **2000**, *287*, 820–825. Available online: https://www.science.org/doi/10.1126/science.287.5454.820 (accessed on 18 June 2025). [CrossRef]
62. Marshall, K.A.; Robertson, M.P.; Ellington, A.D. A biopolymer by any other name would bind as well: A comparison of the ligand-binding pockets of nucleic acids and proteins. *Structure* **1997**, *5*, 729–734. Available online: https://www.sciencedirect.com/science/article/pii/S096921269700227X (accessed on 14 February 2025). [CrossRef]
63. Fischer, N.O.; Tok, J.B.H.; Tarasow, T.M. Massively parallel interrogation of aptamer sequence, structure and function. *PLoS ONE* **2008**, *3*, e2720. Available online: https://journals.plos.org/plosone/article?id=10.1371/journal.pone.0002720 (accessed on 15 May 2025). [CrossRef]
64. Bing, T.; Yang, X.; Mei, H.; Cao, Z.; Shangguan, D. Conservative secondary structure motif of streptavidin-binding aptamers generated by different laboratories. *Bioorg Med. Chem.* **2010**, *18*, 1798–1805. Available online: https://www.sciencedirect.com/science/article/pii/S0968089610000854 (accessed on 30 May 2025). [CrossRef]
65. Mencin, N.; Šmuc, T.; Vraničar, M.; Mavri, J.; Hren, M.; Galeša, K.; Krkoč, P.; Ulrich, H.; Šolar, B. Optimization of SELEX: Comparison of different methods for monitoring the progress of in vitro selection of aptamers. *J. Pharm. Biomed. Anal.* **2014**, *91*, 151–159. Available online: https://www.sciencedirect.com/science/article/pii/S073170851300616X (accessed on 30 May 2025). [CrossRef]
66. Savory, N.; Nzakizwanayo, J.; Abe, K.; Yoshida, W.; Ferri, S.; Dedi, C.; Jones, B.V.; Ikebukuro, K. Selection of DNA aptamers against uropathogenic *Escherichia coli* NSM59 by quantitative PCR controlled Cell-SELEX. *J. Microbiol. Methods* **2014**, *104*, 94–100. Available online: https://www.sciencedirect.com/science/article/pii/S0167701214001791 (accessed on 30 May 2025). [CrossRef]
67. Amilia, N.; Budiarto, B.R.; Mustopa, A.Z.; Aprilian, T.; Manguntungi, B.; Saepudin, E. Isolation of DNA aptamers for Enteropathogenic *Escherichia coli* (EPEC) detection using bacterial-SELEX approach. *HAYATI J. Biosci.* **2022**, *29*, 789–798. Available online: https://journal.ipb.ac.id/index.php/hayati/article/view/39997 (accessed on 30 May 2025). [CrossRef]
68. Tamaian, R. Aptamer-based biosensor design for simultaneous detection of cervical cancer-related microRNAs. *Eng. Proc.* **2023**, *58*, 88. [CrossRef]
69. Zuber, J.; Schroeder, S.J.; Sun, H.; Turner, D.H.; Mathews, D.H. Nearest neighbor rules for RNA helix folding thermodynamics: Improved end effects. *Nucleic Acids Res.* **2022**, *50*, 5251–5262. [CrossRef]
70. Yu, H.; Canoura, J.; Byrd, C.; Alkhamis, O.; Bacon, A.; Yan, A.; Sullenger, B.A.; Xiao, Y. Improving aptamer affinity and determining sequence–activity relationships via Motif-SELEX. *J. Am. Chem. Soc.* **2025**, *147*, 9472–9486. [CrossRef] [PubMed]
71. Hoinka, J.; Zotenko, E.; Friedman, A.; Sauna, Z.E.; Przytycka, T.M. Identification of sequence–structure RNA binding motifs for SELEX-derived aptamers. *Bioinformatics* **2012**, *28*, i215–i223. [CrossRef] [PubMed]
72. Zheng, X.; Hu, B.; Gao, S.X.; Liu, D.J.; Sun, M.J.; Jiao, B.H.; Wang, L.H. A saxitoxin-binding aptamer with higher affinity and inhibitory activity optimized by rational site-directed mutagenesis and truncation. *Toxicon* **2015**, *101*, 41–47. Available online: https://www.sciencedirect.com/science/article/pii/S0041010115001142 (accessed on 30 May 2025). [CrossRef]
73. Dua, P.; Ren, S.; Lee, S.W.; Kim, J.K.; Shin, H.S.; Jeong, O.C.; Kim, S.; Lee, D.K. Cell-SELEX Based identification of an RNA aptamer for *Escherichia coli* and its use in various detection formats. *Mol. Cells* **2016**, *39*, 807–813. Available online: https://www.sciencedirect.com/science/article/pii/S1016847823051051 (accessed on 30 May 2025). [CrossRef]
74. Wu, W.; Zhang, J.; Zheng, M.; Zhong, Y.; Yang, J.; Zhao, Y.; Wu, W.; Ye, W.; Wen, J.; Wang, Q.; et al. An aptamer-based biosensor for colorimetric detection of *Escherichia coli* O157:H7. *PLoS ONE* **2012**, *7*, e48999. Available online: https://journals.plos.org/plosone/article?id=10.1371/journal.pone.0048999 (accessed on 30 May 2025). [CrossRef]
75. Zaitseva, M.; Kaluzhny, D.; Shchyolkina, A.; Borisova, O.; Smirnov, I.; Pozmogova, G. Conformation and thermostability of oligonucleotide d(GGTTGGTGTGGTTGG) containing thiophosphoryl internucleotide bonds at different positions. *Biophys. Chem.* **2010**, *146*, 1–6. Available online: https://www.sciencedirect.com/science/article/pii/S0301462209001987 (accessed on 30 May 2025). [CrossRef]
76. Dougan, H.; Lyster, D.M.; Vo, C.V.; Stafford, A.; Weitz, J.I.; Hobbs, J.B. Extending the lifetime of anticoagulant oligodeoxynucleotide aptamers in blood. *Nucl. Med. Biol.* **2000**, *27*, 289–297. Available online: https://www.sciencedirect.com/science/article/pii/S0969805199001031 (accessed on 30 May 2025). [CrossRef] [PubMed]

77. Bonifacio, L.; Church, F.C.; Jarstfer, M.B. Effect of locked-nucleic acid on a biologically active G-Quadruplex. A structure-activity relationship of the thrombin aptamer. *Int. J. Mol. Sci.* **2008**, *9*, 422–433. [CrossRef] [PubMed]
78. Deng, G.; Zha, H.; Luo, H.; Zhou, Y. Aptamer-conjugated gold nanoparticles and their diagnostic and therapeutic roles in cancer. *Front. Bioeng. Biotechnol.* **2023**, *11*, 1118546. Available online: https://www.frontiersin.org/journals/bioengineering-and-biotechnology/articles/10.3389/fbioe.2023.1118546/full (accessed on 30 May 2025). [CrossRef] [PubMed]
79. Odeh, F.; Nsairat, H.; Alshaer, W.; Ismail, M.A.; Esawi, E.; Qaqish, B.; Bawab, A.A.; Ismail, S.I. Aptamers chemistry: Chemical modifications and conjugation strategies. *Molecules* **2020**, *25*, 3. [CrossRef]
80. Tiwari, A.P.; Ghosh, S.J.; Pawar, S.H. Biomedical applications based on magnetic nanoparticles:DNA interactions. *Anal. Methods* **2015**, *7*, 10109–10120. Available online: https://pubs.rsc.org/en/content/articlelanding/2015/ay/c5ay02334c (accessed on 30 May 2025). [CrossRef]
81. Kotsiri, Z.; Vantarakis, A.; Rizzotto, F.; Kavanaugh, D.; Ramarao, N.; Vidic, J. Sensitive detection of *E. coli* in artificial seawater by aptamer-coated magnetic beads and direct PCR. *Appl. Sci.* **2019**, *9*, 5392. [CrossRef]
82. Filius, M.; Fasching, L.; van Wee, R.; Rwei, A.Y.; Joo, C. Decoding aptamer-protein binding kinetics for continuous biosensing using single-molecule techniques. *Sci. Adv.* **2025**, *11*, eads9687. [CrossRef] [PubMed] [PubMed Central]
83. Ding, Y.; Liu, J. Kinetic ITC of DNA Aptamers Binding for Small Molecules and Implications for Binding Assays and Biosensors. *Chembiochem* **2024**, *25*, e202400225. [CrossRef] [PubMed]
84. Liu, J.R.; Pan, Y.L.; Zhao, Y.P.; Liu, M.C.; Chen, J.H.; Li, C.Y. A colorimetric method for vascular endothelial growth factor detection based on aptamer and magnetic beads. *Nan Fang Yi Ke Da Xue Xue Bao* **2016**, *37*, 210–215. [CrossRef] [PubMed] [PubMed Central]
85. Zhu, S.; Yang, Y.; Li, M.; Yang, Y.; Li, C.; Yin, Y. A pH-responsive bioassay for sensitive colorimetric detection of adenosine triphosphate based on switchable DNA aptamer and metal ion–urease interactions. *Anal. Bioanal. Chem.* **2021**, *413*, 1533–1540. [CrossRef]
86. ALS Environmental. Microbiology: Limit of Detection for Microbiological Analysis. 2017. Available online: https://www.alsenvironmental.co.uk/media-uk/pdf/datasheets/micro-lp/als_micro_limit-ofdetection{-}{-}-microbiology_uk_2017.pdf (accessed on 2 September 2025).
87. Wang, J.; Li, H.; Zhang, X.; Liu, Y. A Portable Colorimetric LAMP Platform for Rapid On-Site Detection of *Escherichia coli* in Environmental Samples. *Sci. Rep.* **2023**, *13*, 14427. [CrossRef]
88. Kaur, H.; Kumar, V.; Singh, A. Advances in Electrochemical and Lateral Flow Aptasensors for Bacterial Detection: Sensitivity, Specificity, and Integration with Portable Platforms. *Nanomaterials* **2024**, *14*, 855. [CrossRef]
89. Zhao, X.; Abubakar, B.; O'Connor, C.; Curtin, J.; Singh, B.; Tian, F. Aptamer-Based Biosensors for Pathogen Detection: Recent Trends and Future Perspectives. *Preprints* **2024**, 2024011268. [CrossRef]
90. USDA Agricultural Research Service. Multiplex Real-Time PCR for Detection of E. coli O157:H7 and Related Pathogens in Water and Food Samples. 2020. Available online: https://www.ars.usda.gov/arsuserfiles/20361500/pdf_pubs/P1810.pdf (accessed on 2 September 2025).
91. Li, J.; Xu, Z.; Chen, W.; Liu, G. A Centrifugal Microfluidic Chip for Rapid, Automated Detection of E. coli in Water Samples. *Biosensors* **2023**, *14*, 313. [CrossRef]